 CMES, vol.95, no.4, pp.283-302, 2013

Numerical Modelling of Liquid Jet Breakup by Different Liquid Jet/Air Flow Orientations Using the Level Set Method

Ashraf Balabel[1]

Abstract: This paper presents the numerical results obtained from the numerical simulation of turbulent liquid jet atomization due to three distinctly different types of liquid jets/air orientations; namely, coflow jet, coaxial jet and the combined coflow-coaxial jet. The applied numerical method, developed by the present authors, is based on the solution of the Reynolds-Averaged Navier Stokes (RANS) equations for time-dependent, axisymmetric and incompressible two-phase flow in both phases separately and on regular and structured cell-centered collocated grids using the control volume approach. The transition from one phase to another is performed through a consistent balance of the interfacial dynamic and kinematic conditions. The topological interfacial changes as well as the geometrical quantities of the interface are predicted by applying the level set method. The results show the formation of the ligaments and its breakup into droplets with different sizes are greatly affected with the liquid/air orientation. The proposed combined coflow/coaxial orientation gives the best spray characteristics represented in final fine droplets. In general, the developed numerical method showed a remarkable capability to predict the primary breakup of the liquid jet. The rational preliminary results obtained give the possibility to extend the performed numerical simulation to predict the secondary atomization regime of the coaxial liquid jet under different operating conditions.

Keywords: Atomization, Coaxial flow, Coflow, Liquid jet, Level set method, Numerical simulation, Turbulence modeling.

[1] Mechanical Engineering Dept., Faculty of Engineering, Taif University, Taif, Hawiyya, 21974, Kingdom of Saudi Arabia.
Corresponding author: Prof. Ashraf Balabel; Email: ashrafbalabel@yahoo.com

1 Introduction

Two phase flow, the simultaneous flow of two phases or two immiscible liquids within common interface, has a wide range of engineering as well as industrial applications. For major interest for aerodynamic applications are the more complicated liquid-gas flows that are characteristics for bubble and droplet dynamics [Fuster, Agbaglah, Josserand, Popinet and Zaleski (2009)], atomization and spray of liquid jet [Lefebvre (1989)], and other multiphase flow systems [Kolev (2007)]. Due to the importance of jet dynamics in most of atomization systems, there is an increased attention being given for the prediction of evolution and breakup of liquid jets either numerically, analytically or experimentally.

It is well known that the combustion efficiency in diesel engines, gas turbine engines, oil burners and liquid rockets is strongly dependent on liquid fuels atomization process [Yang, Habiballah, Hulka and Popp (2004)]. Consequently, atomization process remains a challenging topic of research [Linne, Paciaroni, Hall, and Parker (2006)]. Turbulence usually interacts with other atomization mechanisms, such as surface instabilities, ligament formation, stretching and fragmentation to transform large scale coherent liquid structures into small scale droplets. Generally, atomization process that occurs in a turbulent environment usually includes a wide range of time and length scales [Menard, Tanguy and Berlemont (2006)].

The numerical investigations of the atomization process are scarcely due its computational challenges [Desjardins, Moreau and Pitsch (2008)]. Disturbances, which cause breakup of liquid jet, include: rapid acceleration, high shear stresses and turbulent fluctuations. Moreover, in turbulent flow fields, the break-up of the liquid jet is controlled by the pressure fluctuations of a turbulent motion. The hydrodynamic fluctuations of the pressure are caused by velocity changes. As proposed in [Hinze (1959)], only the energy associated with eddies with smaller length scales is available to case disintegration, however, larger eddies merely transport the liquid ligaments and droplets formed.

Although several papers have recently reported experimental efforts to understand the physics of the liquid jet breakup, ligaments and droplets formation and its related dynamics in turbulent flow, however, experimental measurements and the observation of dense and small region with high spatial-temporal resolution in such applications have been difficult [Eggers (1997)].

Analytically, where the governing equations of liquid jet are solved in an exact or approximate way obtaining a mathematical expression for the most important physical quantities, nearly complete information regarding the flow field is obtained. This approach is not always feasible because the difficulties associated with the solution of the governing equations, especially, in turbulent flow [Schlichting (1979)].

More recently, the carefully executed numerical simulations in such context can virtually replace experiments. In general, the numerical predictions of turbulent jet dynamics have been limited in accuracy partly by the development and the performance of three key elements, viz.: development of the computational algorithm, interface tracking methods, and turbulence models.

During the last decade, a variety of computational fluid dynamics techniques have been developed to study turbulent two-phase flow dynamics. A comprehensive review of the numerical models applied for two-phase flow up to 1996 can be found in [Crowe, Troutt and Chung (1996)]. More extended review up to 2010 for the atomization process and its related dynamics can be found in [Shinjo and Umemura (2010)].

In the numerical simulation of turbulent jet dynamics, it has been difficult to predict the physical processes occurred due to the requirement of high resolution, especially for high Weber and Reynolds numbers. The severe resolution required in such simulation is essentially in order to resolve the important role played by surface tension in ligament and drop formation. Consequently, in order to obtain an insight in such complex dynamics, the numerical treatments of such processes are carried out in a number of sequential steps starting from the investigation of the surface instability that leads to ligament deformation followed by droplet formation and drop separation from a single ligament till the secondary break-up of liquid droplets.

The application of Direct Numerical Simulation (DNS) in two-phase turbulent flow is currently in the primitive stage as it is limited to relatively low Reynolds number and simple geometries [Shinjo and Umemura (2010)]. Consequently, resolving all physical processes in such context is not possible. Although Large Eddy Simulation (LES) has been developed to form a bridge between Reynolds-Averaged Navier-Stokes equations (RANS) and DNS [Rgea, Bini, Fairweather and Jones (2009)], there has not been much of an effort to employ LES for modelling turbulent two-phase flow. In most cases, LES can be directly used in turbulent two-phase flow, provided that the fluids interface does not undergo any significant deformation during the evolution. However, the presence of a rapidly changing of the fluids interface has relatively unknown effects on LES. It is possible that the deformation of the interface has a dynamic interaction with both the resolved and modelled turbulence scales in the flow. At the same time, it is also possible that the modelling of turbulent phenomena by LES has consequences in the computation of the interface dynamics.

The fact that a generally applicable model for turbulence in single-phase flows is not yet available compounds the problem for two-phase turbulent flow. However, RANS type turbulence models with the linear eddy-viscosity models (LEVM),

which based on Boussinesq assumption, are still standard in many practical engineering applications.

Among several LEVM, the standard (STD) k-ε turbulence model [Launder and Spalding (1974)] is still the most widely used in industrial and engineering applications as it represents a good comparison between accuracy and computational efficiency. It was developed; calibrated and validated to cover a wide range of industrial and engineering applications. It is a robust two-equation turbulence model and it yields quite reasonable results in high Reynolds number flow when its restrictions are undertaken. Therefore, the two-equation STD k-ε model has been the subject of much research in the last years. Therefore, in the present work; the STD k-ε turbulence model is applied to predict the jet dynamics in turbulent flow regime.

Usually, in the numerical simulation of turbulent two-phase flow, the Navier-Stokes equations are coupled to one of the available tracking methods in order to predict the complex topological changes of the phase interface. Given examples for such tracking methods, Volume-Of-Fluid (VOF) method [Nichols and Hirt (1975)] and Level Set Method (LSM) [Osher and Sethian (1988)] are the most popular interface capturing methods. Although the VOF method has been widely applied for predicting different complex two-phase flows, it suffers from several numerical problems such as interface reconstruction algorithms and the difficult calculation of the interface curvature [Zhaorui, Jaberi1 and Shih (2008)]. These numerical problems can, in particular, limit the accuracy and the stability of the numerical method adopted for calculation of two-phase flows, especially when the surface tension is included. A comprehensive review for the different VOF methods and their numerical constraints can be found in [Scardovelli, Zaleski (1999)].

In contrast to the VOF methods, the level set methods offer highly robust and accurate numerical technique for capturing the complex topological changes of moving interfaces under complex motions. The basic idea of LSM is the use of a continuous, scalar and implicit function defined over the whole computational domain with its zero value is located on the interface. The LSM divides the domain into grid points that contain the value of the scalar function; therefore, there is an entire family of contours. The interface is then described as a signed distance function at any time and, consequently, the geometric properties of the highly complicated interfaces are calculated directly from level set function. Moreover, the complex topological changes of interfaces such as merging and breaking-up are handled automatically in a quite natural way without any additional procedure. In addition, the extension of the LSM to three-dimensional problems is easy and straightforward.

Referring to the previous discussion, the LSMs have seen tremendously in different CFD-applications of diverse areas, e.g. two-phase flows, turbulent atomization,

grid generation and turbulent combustion [Peters (2000)]. However, the LSMs suffer from numerical diffusion which may cause a smoothing out of sharp edges of interface. The level set function is usually evolved by a simple Eulerian scheme and, consequently, the final implementation of LSM does not provide full volume conservation, so highly accurate transport schemes are required. In our previous work [Balabel, Binninger, Herrmann and Peters (2002)], a new technique for solving the level set equation has been developed and validated by performing a number of challenge test cases.

In more particular, recently the numerical simulation of the coaxial liquid jet is of important interest due to its wide range applications and challenges. Phenomenological studies of coaxial liquid oxygen atomized by a fast, coaxial gaseous hydrogen jet under a broad variation of influencing parameters including injector design, inflow, and fluid conditions are performed in [Mayer (1994)]. Recently, Spray formation was simulated in Ansys CFX under a Lagrangian model. The primary breakup Blob model is used to handle atomization of the liquid while the secondary breakup TAB and ETAB models are evaluated for the subsequent breakup of the atomized droplets [Fung, Inthavong, Yang and Tu (2009)]. More recently, a Large Eddy Simulation is applied to predict the mixing and the intermittency of coaxial turbulent jet discharging into an unconfined domain [Dinesh, Savill, Jenkins and Kirkpatrick (2010)]. In a coaxial shear injector element relevant to liquid propellant rocket engines, a numerical simulation for liquid water issued into nitrogen gas at elevated pressures is performed [Ibrahim, Kenny and Walker (2010)]. It ca be concluded from such literature review that, the numerical simulation of coaxial liquid jets is few and required further improvement and continuation.

Consequently, in the present paper, the developed numerical method on the basis of the control volume approach is applied to predict the coaxial jet dynamics. The level set method predicts the interfacial evolution of the jet and the related formation, deformation and breakup of ligaments and drops. The complete system of the governing equations and the associated numerical models and boundary conditions are described in details in the following sections.

2 Physical and Mathematical formulation

The governing equations for 2D unsteady, axisymmetric, isothermal and incompressible turbulent two-phase flow are described in the present section. The system of the governing equations is based on the known RANS equations which stand for the Reynolds-averaged Navier Stokes equations. The standard two-equation STD k-ε turbulence model is applied for predicting the turbulence characteristics. The level set method is adopted for describing the topological changes of the coaxial liquid jet. Consequently, the associated boundary conditions and the numerical al-

gorithms and models applied for solving the appropriate governing equations are also discussed.

The physical domain of the coaxial jet to be solved numerically is shown in figure 1. The governing equations are solved numerically using the control volume approach organized over the computational domain shown in figure 2.

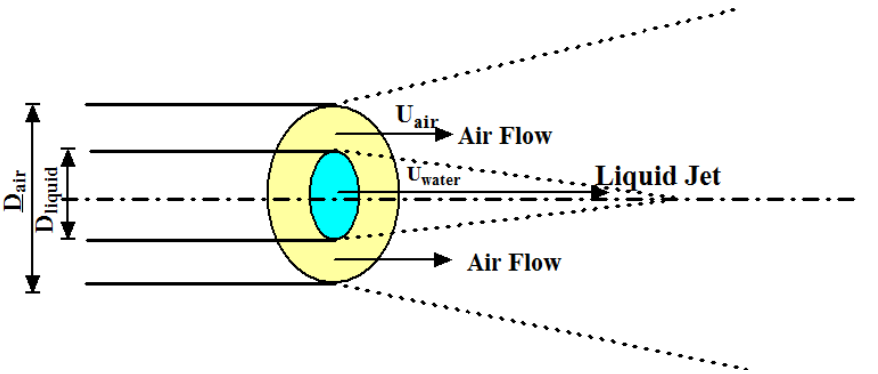

Figure 1: The physical domain of the coaxial jet

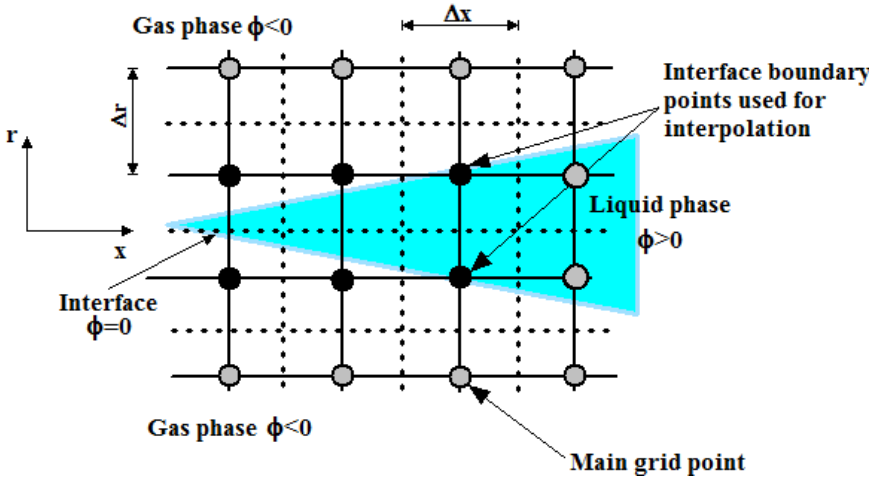

Figure 2: The computational domain of the coaxial jet problem

2.1 Reynolds-Averaged Navier-Stokes Equations

The Reynolds form of the continuity and momentum equations for turbulent two-phase flow, called here RANS equations, at each point of the flow field can be represented by the following equations after neglecting the body force:

$$\nabla \cdot (\rho \bar{u})|_{\alpha} = 0 \tag{1}$$

$$\frac{\partial(\rho \bar{u})}{\partial t} + \nabla \cdot (\rho \overline{uu}) + \nabla p = \nabla \cdot (2\mu \hat{S} + \hat{\Re}_t)\Big|_{\alpha} \tag{2}$$

where the subscript α takes the values 1 and 2 and denotes the properties corresponding to the liquid and gas phases, respectively. In the above system of equations, $\bar{u}$ is the velocity vector, p is the pressure, ρ is the density, μ is the molecular viscosity, $\hat{S}$ is the strain rate tensor and $\hat{\Re}_t$ is the turbulent stress tensor which are given as:

$$S_{ij} = 0.5(\frac{\partial u_i}{\partial x_j} + \frac{\partial u_j}{\partial x_i}) \tag{3}$$

$$\Re_{ij} = -\rho \overline{u_i' u_j'} = -\frac{2}{3}\rho k \delta_{ij} + 2\mu_t S_{ij} \tag{4}$$

where δ_{ij} is the Kronecker delta and $\overline{u_i' u_j'}$ are the average of the velocity fluctuations. The turbulent viscosity is defined as:

$$\mu_t = \rho C_\mu k^2/\varepsilon \tag{5}$$

The turbulent kinetic energy k and its dissipation rate ε can be estimated by solving the following equations:

$$\frac{\partial(\rho k)}{\partial t} + \nabla \cdot (\rho k \bar{u}) = \nabla \cdot (\mu + \mu_t/\Sigma_k)\nabla k + 2\mu_t \hat{S}\hat{S} - \rho\varepsilon \tag{6}$$

$$\frac{\partial(\rho \varepsilon)}{\partial t} + \nabla \cdot (\rho \varepsilon \bar{u}) = \nabla \cdot (\mu + \mu_t/\Sigma_\varepsilon)\nabla \varepsilon + (2C_{1\varepsilon}\mu_t \hat{S}\hat{S} - C_{2\varepsilon}\rho\varepsilon)\varepsilon/k \tag{7}$$

The coefficients for the so-called STD k-ε turbulence model are given as follows [Launder and Spalding (1974)]:

$$C_\mu = 0.09, \Sigma_k = 1, \Sigma_\varepsilon = 1.3, C_{1\varepsilon} = 1.44, C_{2\varepsilon} = 1.92$$

2.2 Level Set Function

The level set method is a class of capturing method where a smooth phase function φs is defined over the complete computational domain. The level set function at any given point is taken as the signed normal distance from the interface separates the two fluids with positive on one side (i.e. $\varphi >$ w), and negative on the other (i.e. $\varphi <$ w). Consequently, the interface is implicitly captured as the zero level set of the level set function, as shown in figure 1. This level set function is updated with the computed velocity field and thus propagating the interface.

The update of the level set function with time can be determined by solving the following transport equation:

$$\frac{\partial \varphi}{\partial t} + \bar{u} \cdot \nabla \varphi = 0 \tag{8}$$

where $\bar{u}$is the velocity vector. Since the interface is captured implicitly, the level set algorithm is capable of capturing the intrinsic geometrical properties of highly complicated interfaces in a quite natural way. Consequently, the normal vector and the curvature of the interface can be defined as:

$$\bar{n} = \frac{\nabla \varphi}{|\nabla \varphi|}, \qquad \kappa = \nabla \cdot \bar{n} \tag{9}$$

The time-stepping procedure for the level set equation is based on the second-order Runge-Kutta method. An important step in the solution algorithm of the level set function is to maintain the level set function as a distance function within the two fluids at all times, especially near the interface region, *i.e.*the Eikonal equation; $|\nabla \varphi| = 1$ should be satisfied in the computational domain. This can be achieved each time step by applying the re-initialization algorithm described in [Sussman, Smereka and Osher (1994)] for a specified small number of iterations.

Since the development of the level set method for incompressible two-phase viscous flow [Sussman, Smereka and Osher (1994)], a large number of articles on the subject have been published and several types of problems have been tackled with this method; see for instance the cited review [Sethian and Smereka (2003)]. However, the implementation of the level set method in predicting the moving interfaces under turbulent characteristics is indeed very scarce.

2.3 Interfacial Stress Modelling

The jump conditions at the interface separating the two fluids are comprised of the dynamic and kinematic conditions. In the case of two immiscible fluids, taking the projections of the jump conditions in the directions normal and tangential to the

interface and considering a constant surface tension, one obtains the following two equations in the normal and tangential directions, respectively:

$$[p - 2\mu_{eff}(\nabla \mathrm{u} \cdot \mathrm{n}) \cdot \mathrm{n}] = \sigma \kappa \mathrm{n} \tag{10}$$

$$[\mu_{eff}(\nabla \mathrm{u} \cdot \mathrm{n}) \cdot \mathrm{t} + \mu_{eff}(\nabla \mathrm{u} \cdot \mathrm{t}) \cdot \mathrm{n}] = 0 \tag{11}$$

where σ is the surface tension, $\mu_{eff} = \mu + \mu_t$ is the effective viscosity, κ is the curvature of the interface, **n** and **t** is the normal and tangential vector to the interface. It is noticed from the above equations that surface tension effects are included in the normal stress balance, while the equality of the shear stress is satisfied in the tangential direction.

The idea of our modeling is straightforward. By introducing a number of so called "Interfacial Markers" on the intersection points of computational grids with the interface, the interfacial stresses are computed at such markers and then it is used to drive the liquid phase through the momentum equations Moreover, at the position of the interfacial markers, the local curvature is easily estimated by means of a simple interpolation technique. Once the curvature is known the surface tension force is evaluated.

The present surface tension model ensures that both the pressure calculated within the liquid phase and the surface tension pressure is consistent and dynamically similar, as their effect is determined in the same way. Accordingly, the pressure drop across the interface cancels exactly the surface tension potential at the interface.

For more generality of the present model, see figure 1, it is considered that the interfacial pressure at the liquid phase p_l is determined by evaluating the pressure in the gas phase p_g and the surface tension pressure, i.e.:

$$p_l = p_g + \sigma \kappa \tag{12}$$

The pressure values calculated from the above equation are then used as Dirichlet boundary conditions for solving the Poisson equation for the pressure. The above interfacial conditions are known as Laplace's formula [Brackbill, Kothe and Zemach (2002)] for the surface pressure in case of inviscid incompressible fluids with constant surface tension coefficient. Moreover, in addition to the equality of the dynamically interfacial stresses described above, the kinematic conditions should also be considered. When there is no mass transfer through the interface, the kinematic conditions is satisfied at the moving interface by assuming the continuity of the normal velocity component;

$$V_n|_l = V_n|_g \tag{13}$$

However, in case of stationary interface, the normal velocity must equal zero. Satisfying the previous interfacial boundary conditions is an important task in the numerical simulation of two-phase flows as the pressure and velocity field inside the liquid phase are caused by the external gas field. Therefore, the exact pressure level inside the liquid phase, which considered as the driving force, should be accurately specified.

2.4 IMLS Numerical Scheme

The present algorithm is based on the implicit fractional step-non iterative method to obtain the velocity and pressure filed in the computational domain. Assuming that the velocity field reaches its final value in two stages; that means

$$U^{n+1} = U^* + U_c \tag{14}$$

whereby, U^* is an imperfect velocity field based on a guessed pressure field, and U_c is the corresponding velocity correction. Firstly, the 'starred' velocity will result from the solution of the momentum equations. The second stage is the solution of Poisson equation for the pressure:

$$\nabla^2 p_c = \frac{\rho_\alpha}{\Delta t} \nabla \cdot U^* \tag{15}$$

where Δt is the prescribed time step and p_c is called the pressure correction. Once this equation is solved in each phase, one gets the appropriate pressure correction and, consequently, the velocity correction is obtained according to the following equation:

$$U_c = -\frac{\Delta t}{\rho_\alpha} \nabla p_c \tag{16}$$

This fractional step method described above ensures the proper velocity-pressure coupling for incompressible flow field. However, the accurate solution of the surface pressure occurring at transient fluid interfaces of arbitrary and time dependent topology enables an accurate modeling of two- and three dimensional fluid flows driven by surface forces. Assuming that a square regular mesh is used for the calculation, the curved shape of the interface causes unequal spacing between the interface and some internal grid points, as illustrated in figure 3. In the present work, a linear interpolation is used to assign values of the curvature at the interface from the known internal grid points values.

Referring to figure 2, the interphase boundary value of the curvature can be calculated according to the following relation:

$$\kappa_b(\varphi) = (1-f)\kappa_P(\varphi) + f\kappa_B(\varphi), \qquad f = \varphi_P/(\varphi_P - \varphi_B) \tag{17}$$

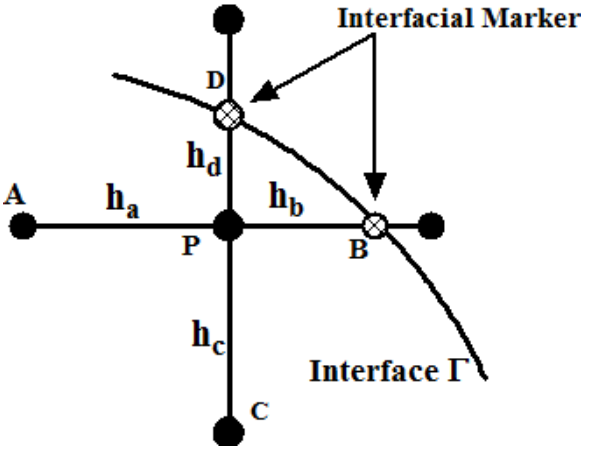

Figure 3: Calculation of the interphase boundary values.

The calculation of the local curvature at the interfacial markers enables us to calculate the surface tension force, i.e. the surface pressure. Consequently, an approximation of the Poisson equation for pressure at point **p** can be represented as follows:

$$p_{ij} = \left[\frac{p_a}{h_a(h_a+h_b)} + \frac{p_b}{h_b(h_a+h_b)} + \frac{p_c}{h_c(h_c+h_d)} + \frac{p_c}{h_d(h_c+h_d)} + S_p \right]$$

where S_p is the source term described in Eq. (12). The above equation can be developed utilizing Taylor-series expansion about the grid point **p**. It can easily be shown that the above formula is equivalent to that in case of a regular grid formula if the distances $h_a = h_b = \Delta x$,and $h_c = h_d = \Delta y$. More details about the numerical procedure used to solve the above system of equations can be found in [Balabel (2002), (2011), (2011), (2012), (2012), (2012), (2012)]

The above algorithm is applied in a separate way in both phases to obtain the fluid variables in each phase. By using the velocity and pressure values on the gas phase as a boundary conditions defined on the interface, the solution of the liquid phase is carried out. After that, the turbulent equations are solved on both phases simultaneously. The normal velocity at the interface is then used to move the interface using the level set approach and to obtain its topological changes. Consequently, the whole algorithm is repeated until it would reach the statistically steady state condition.

3 Results and Discussion

In the present section, three different cases are considered for showing the effect of liquid/air orientation on the breakup mechanism of the liquid jet issued with a constant velocity 50m/s. The configuration and the boundary conditions of the computational domain are shown in figure 4.

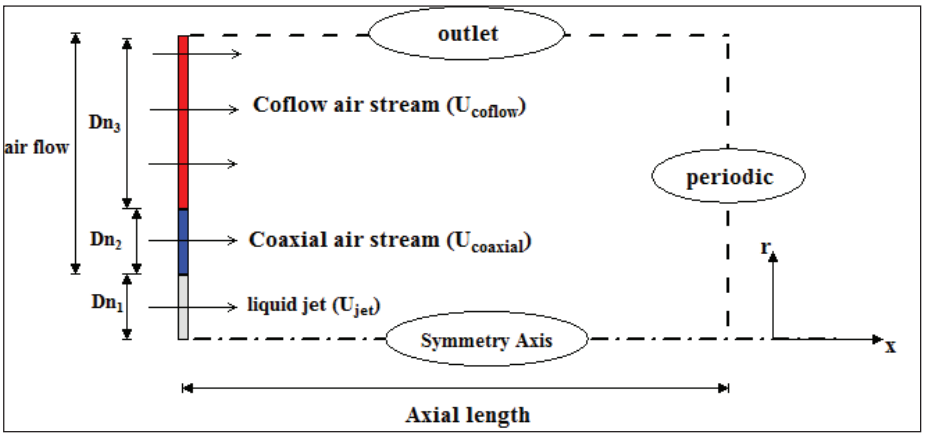

Figure 4: Configuration of the computational domain and boundary conditions.

The input data of the numerical simulation for the three cases considered are shown in Table 1 and the liquid air properties are shown in Table 2.

Table 1: The initial and input data for numerical simulation

	U_{jet}	$U_{coaxial}$	U_{coflow}	Dn_1	Dn_2	Dn_3	Axial length
Case I	50 m/s	0.0	150 m/s	0.05 m	0.	0. 1m	0.15 m
Case II	50 m/s	250 m/s	0.0	0.05 m	0.025 m	0.	0.15 m
Case III	50 m/s	250 m/s	150 m/s	0.05 m	0.025 m	0. 075m	0.15 m

3.1 Ligament shape and formation

Figure 4 shows the formation and deformation of the ligaments formed at the interface separating the two streams as a result of the aerodynamic forces represented in the relative velocity and the two streams orientations. It can be seen that the ligament formed in Case I is more elongated in the axial stream direction due to

Table 2: Property of Air and Liquid used for simulation

Property	Air flow	Liquid Jet
Density	1.0 kg/m^3	2 kg/m^3
Viscosity	1.5e^{-5} Pa. s	1.5e^{-3} Pa.s
Surface tension	0.	0.02 N.m
Initial pressure	1 bar	1 bar

the effect of the coflow stream. However, the enrollment process of the deformed ligament, or the so called Kelvin-Helmholtz instability can be seen clearly in Case II and much more visible in Case III. This enrollment process is prior to the droplet breakup in liquid jet atomization process. The time required for preparing the deformed ligament to the initial primary breakup process is faster in Case II and Case III than the coflow jet case.

3.2 Fragmentation and primary breakup

The primary breakup is usually occurred when the liquid ligaments detach from the liquid surface and moves in irregular way. The spray properties usually decide the shape and the size of the formed liquid ligaments. Figure 5 shows the fragmentation process of liquid ligaments for the three cases considered. In Case I, the liquid ligaments detach and moves further in the downstream direction due the coflow effect. The size of the ligaments is appeared to be relatively small compared with the bulk liquid. In later time steps, these ligaments may be further break or collides with each other or with the bulk liquid. The formation of droplets from such case is seen to be relatively complex. However, the liquid jet can posses a large penetration due to the velocity of the coflow air stream.

In Case II, the enrolling process of the initial Kelvin-Helmholtz instability may retard the detachment process of the liquid ligaments. This phenomenon is related to the high relative velocity and the interfacial stresses encountered in coaxial liquid jets. The formation of small droplets resulting fro detached ligaments can be seen in later time steps and the liquid core is seen to be thinner compared with the previous case.

In Case III, the process is more regular where the ligaments formed are detached faster from the liquid surface and go through further breakup process forming small droplets.

In general, the time required for obtaining fine droplets is relatively small in Case III in comparison with the other cases.

3.3 Droplet formation and secondary breakup

Figure 6 shows the formation of the droplets from the breakup of the liquid ligaments, which known as the secondary breakup process. As can be seen from the previous discussion, the secondary process is dependent on the preceding processes of ligament formation and detachment. Consequently, it is predicted that the secondary breakup process is more efficient and faster in Case III than Case II and Case I. This leads to an efficient atomization process with preferred characteristics.

Table 3: Time steps used for plotting Figure 5

	t_1(s)	t_2(s)	t_3(s)	t_4(s)	t_5(s)
Case I	0.	0.0039	0.0079	0.012	0.014
Case II	0.	0.0011	0.022	0.0034	0.0049
Case III	0.	0.0011	0.0023	0.0036	0.0052

Table 4: Time steps used for plotting Figure 6

	t_1(s)	t_2(s)
Case I	0.018	0.23
Case II	0.0085	0.13
Case III	0.0078	0.0094

Table 5: Time steps used for plotting Figure 7

	t_1(s)	t_2(s)
Case I	0.032	0.36
Case II	0.0137	0.23
Case III	0.011	0.14

4 Conclusion

Three different types of liquid jets/air orientations are numerically simulated and the obtained results are discussed in details. The three distinctly different types namely, coflow jet, coaxial jet and the combined coflow-coaxial jet. The developed numerical method is based on the solution of the Reynolds-Averaged Navier

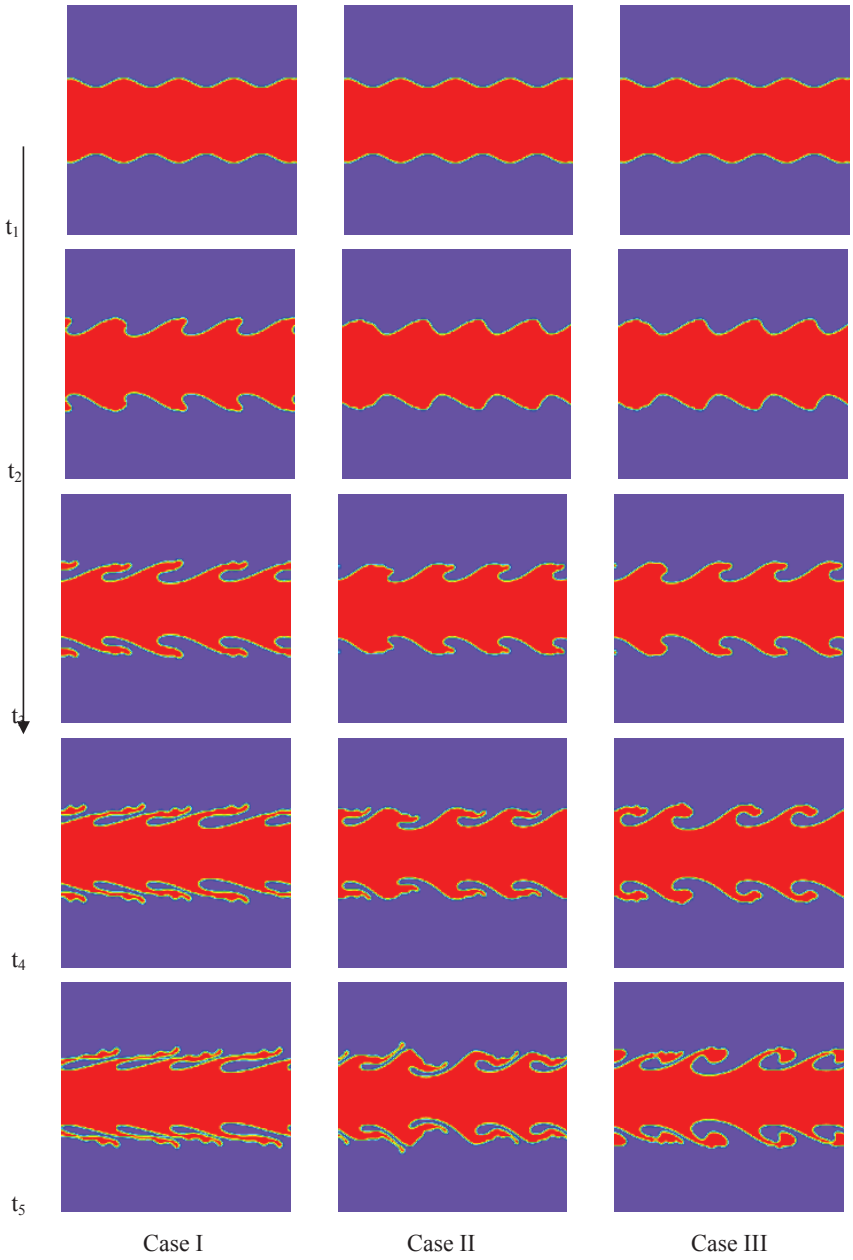

Figure 5: The formation and deformation of ligament prior to the breakup for the three cases considered at different times shown below in Table 3

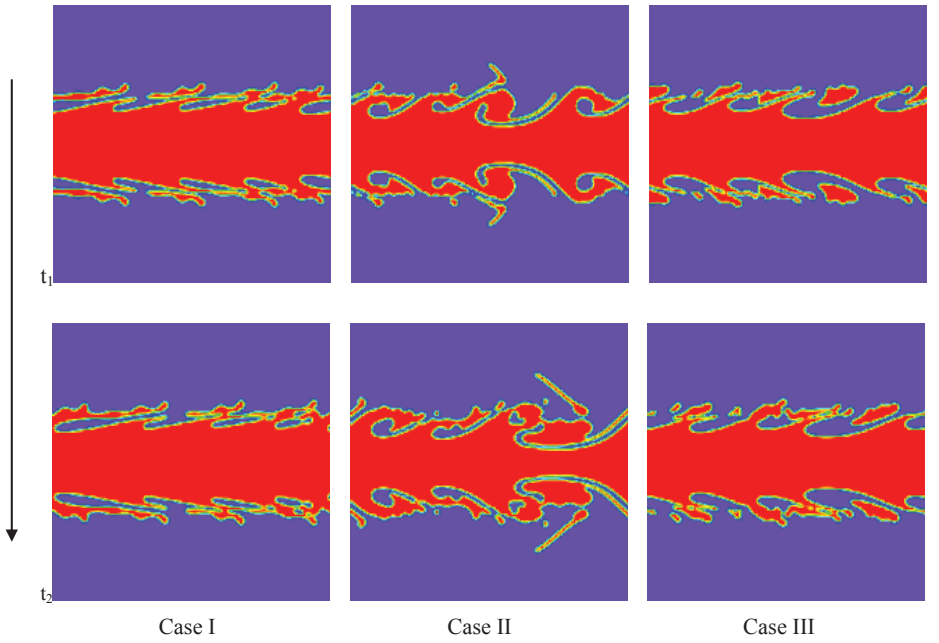

Figure 6: Ligament fragmentation and primary breakup process for the three cases considered at different times shown below in Table 4

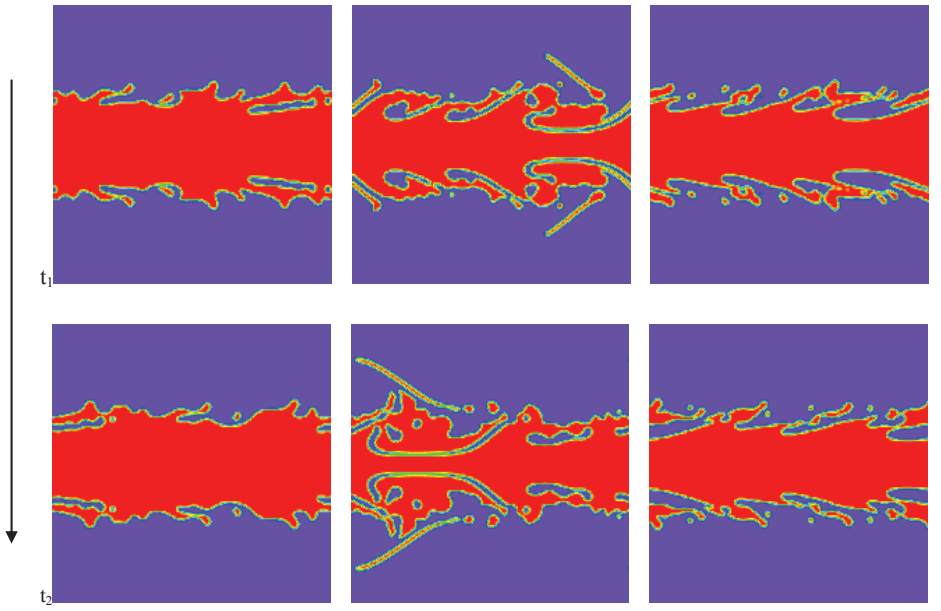

Figure 7: Secondary breakup process of formed droplets for the three cases considered at different times shown below in Table 5.

Stokes (RANS) equations for time-dependent, axisymmetric and incompressible two-phase flow in both phases separately and on regular and structured cell-centered collocated grids using the control volume approach. The topological changes of the interface separating the two streams are predicted by applying the level set method. The results indicate the effects of liquid/air orientation on the formation of the ligaments and its breakup into droplets with different sizes. The proposed combined coflow/coaxial orientation showed the best spray characteristics represented in final fine droplets primary as well as secondary breakup.

In general, the developed numerical method showed a remarkable capability to predict the primary breakup of the liquid jet. In the future, we are planning to extend the developed numerical method to predict the secondary atomization regime of the coaxial liquid jet under different operating conditions.

5 References

Balabel, A. (2012): Numerical simulation of two-dimensional binary droplets collision outcomes using the level set method. *International Journal of Computational*

Fluid Dynamics, vol. 26, no. 1, pp. 1-21.

Balabel, A. (2012): Numerical modeling of turbulence-induced interfacial instability in two-phase flow with moving interface. *Applied Mathematical Modelling*, vol. 36, pp. 3593–3611.

Balabel, A. (2012): A Generalized Level Set-Navier Stokes Numerical Method for Predicting Thermo-Fluid Dynamics of Turbulent Free Surface. *Computer Modeling in Engineering and Sciences (CMES)*, vol.83, no.6, pp.599-638.

Balabel, A. (2012): Numerical Modelling of Turbulence Effects on Droplet Collision Dynamics using the Level Set Method. *Computer Modeling in Engineering and Sciences (CMES)*, vol.89, no.4, pp.283-301.

Balabel, A. (2011): On the performance of linear and nonlinear k–ε turbulence models in various jet flow applications. E*uropean Journal of Mechanics B/Fluids*, vol. 30, pp. 325–340.

Balabel, A. (2011): Numerical prediction of droplet dynamics in turbulent flow, using the level set method. *International Journal of Computational Fluid Dynamics*, vol. 25, no. 5, pp. 239-253.

Balabel, A.; Binninger, B.; Herrmann, M.; Peters, N. (2002): Calculation of Droplet Deformation by Surface Tension Effects using the Level Set Method. *Combust. Sci. Technology*, vol. 174, no. 11-12, pp. 257–278.

Crowe, C. T.; Troutt, T. R.; Chung, J. N.(1996): Numerical models for two-phase turbulent flows. *Annu. Rev. Fluid Mech.*, vol. 28, pp. 11-43.

Desjardins, O.; Moureau, V.; Pitsch, H. (2008): An accurate conservative level set/ghost fluid method for simulating turbulent atomization. *Journal of Computational Physics*, vol. 227, pp. 8395–8416.

Dinesh, K. R.; Savill, A.; Jenkins, K.; Kirkpatrick, M. (2010): A study of mixing and intermittency in a coaxial turbulent jet. *Fluid Dynamics Research*, vol. 42, no. 2, pp. 1-40.

Eggers, J. (1997): Nonlinear Dynamics and Breakup of Free-Surface Flow. *Rews. Modern Phys.*, vol. 69, no. 3, pp. 865–929.

Fung, M. C.; Inthavong, K.; Yang, W.; TU, J. (2009): External characteristics of spray atomisation from a nasal spray device. *Seventh International Conference on CFD in the Minerals and Process Industries CSIRO, Melbourne*.

Fuster, D.; Agbaglah, G.; Josserand, C.; Popinet, S.; Zaleski, S. (2009): Numerical simulation of droplets, bubbles and waves: state of the art, *Fluid Dyn. Res.* vol. 41, pp. 1-24.

Hinze, J. O. (1959): *Turbulence*, New York, McGraw-Hill.

Ibrahim, E.; Kenny, J.; Walker, N. (2010): Atomization of coaxial liquid jets. *Applied Physical Research*, vol. 2, no. 1, pp. 3-18.

Kolev, N. I. (2007): *Multiphase flow dynamics: Thermal and Mechanical Interaction*, Springer.

Launder, B. E.; Spalding, D. B. (1974): The numerical computation of turbulent flow. *Computer Methods in Applied Mechanics and Engineering*, vol. 3, no. 2, pp. 269-289.

Lefebvre, A. H. (1989): *Atomization and sprays*, Hemisphere Publishing Corporation.

Li, Z.; Jaberi, F. A.; Shih, T. (2008): A hybrid Lagrangian–Eulerian particle-level set method for numerical simulations of two-fluid turbulent flows. *Int. J. Num. Methods in Fluids*, vol. 56, pp. 2271-2300.

Linne, M.; Paciaroni, M.; Hall, T.; Parker, T. (2006): Ballistic imaging of the near field in a dense spray. *Exp. Fluids*., vol. 49, no. 4, pp. 911-923.

Mayer, W.(1994): Coaxial atomization of a round liquid jet in a high speed gas stream: A phenomenological study. *Experiments in Fluids*, vol. 16, pp. 401-410.

Menard, T.; Tanguy, S.; Berlemont A. (2007): Coupling level set/VOF/ghost fluid methods: Validation and application to 3D simulation of the primary break-up of a liquid jet. *Int. J. Multiphase Flow*, vol. 33, pp. 510-524.

Nichols, B. D.; Hirt, C. W. (1975): Methods for calculating multi-dimensional, transient free surface flows past bodies. *Proc. First Int. Conf. Num. Ship Hydrodynamics Gaithersburg,* pp. 20–23.

Osher, S.; Sethian, J. A. (1988): Fronts propagating with curvature-dependent speed: algorithms based on Hamilton–Jacobi formulations. *Journal of Computational Physics*, vol. 79, pp. 12–49.

Peters, N. (2000): *Turbulent combustion*. Cambridge University Press, Cambridge, UK.

Rgea, S.; Bini, M.; Fairweather, M.; Jones, W. P. (2009): RANS modelling and LES of a single-phase, impinging plane jet. *Computer and Chemical engineering*, vol. 33, pp. 1344-1533.

Scardovelli, R.; Zaleski, S. (1999): Direct numerical simulation of free-surface and interfacial flow. *Annu. Rev. Fluid Mech.,* vol. 31, pp. 567–603.

Schlichting, H.(1979): *Boundary Layer Theory*, McGraw-Hill | ISBN: 0070553343.

Shinjo, J.; Umemura, A. (2010): Simulation of liquid primary breakup: Dynamics of ligament and droplet formation. *Int. J. Multiphase Flow*, vol. 36, no. 7, pp. 513-532.

Yang, V.; Habiballah, M.; Hulka, J.; Popp, M. (2004) Liquid Rocket Thrust Chambers: Aspects of Modeling, Analysis, and Design. *American Institute of Aeronautics and Astronautics, Inc*.